Accuracy and Robustness Evaluations on Algorithms of Ultrasonic Spinning Rheometry

Taiki Yoshida, Yuji Tasaka, Hyun Jin Park, and Yuichi Murai
Laboratory for Flow Control, Faculty of Engineering, Hokkaido University, Japan

We present a novel methodology using ultrasonic velocity profiling (UVP) to overcome some fatal problems in conventional torque rheometry, such as shear banding, wall-slip, viscoelastic instabilities, and so on. Termed ultrasonic spinning rheometry, the methodology can evaluate rheological properties from unsteady simple shear flows in a rotational cylindrical vessel. Different algorithms have applied to various kinds of fluids to evaluate the properties, there is, however, no trials on accuracy and robustness evaluations for the algorithms yet. We investigated apparent noise characteristics of velocity distributions in our measurement system and examined statistical calculations of effective viscosity profiles analyzing velocity profiles simulated by a numerical solution with artificial random noise.

Keywords: Rheometry, Newtonian viscosity, Accuracy evaluation, Error analysis, Shear flow

1. Introduction

In the present industry, it is of great importance not only to comprehend fluid-product properties but also to deal with the fluid material in the producing systems. The complete comprehension of rheology has great significance to enhance and keep the products quality. Rheometry which quantitatively evaluates shear-rate dependent properties has been studied and developed to deal with complex fluids, such as dense suspensions, bubbly liquids, etc. Conventional rheometry using torque measurements are widely used in the industry and can evaluate the properties of test materials when deformations of the materials accord with the theory. There are many complications due to non-Newtonian characteristics, although most industrialized fluid products are included in the non-Newtonian fluids. The complications occur measurement limitations in the application to complex fluids. The most dominant factor is called the “Couette inverse problem” [1], which is caused by ambiguities of knowledge in “local” deformations of non-Newtonian fluids. To overcome the problems, a rheometry coupled with velocimetry are desired as a novel approach, hence UVP [2] has great advantages of wide applicability due to high spatiotemporal resolution.

We proposed a rheometry using UVP for complex fluids in rotating cylindrical systems without requiring an inner cylinder to measure the axial torque, termed ultrasonic spinning rheometry (USR). This rheometry performs rheological evaluations, such as effective viscosity, shear modulus, linear viscoelasticity, yield stress, etc. Analytical procedures of USR (Fig. 1) have been developed in our previous works [3−9]. Yoshida *et al.* [7] reported an algorithm to measure effective viscosity using the phase-lag analysis, and Yoshida *et al.* [9] revealed macro-rheological properties of clay dispersions using the phase-lag analysis. Since there are still no detailed evaluations of the accuracy of the method, in this report, accuracy on viscosity measurement of USR is evaluated by velocity profiles of the analytical solution with artificial random noises. To investigate the accuracy by calculating statistically, O (10^3 − 10^4) trials are performed by iterative calculations.

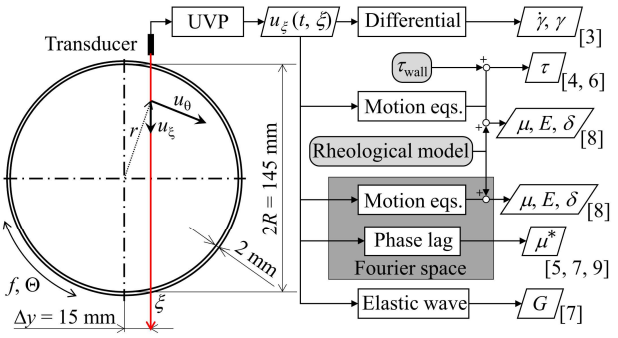

Figure 1: Schematic of the experimental setup in the arrangement of the ultrasonic transducer to a cylindrical container, and flow diagram of details of analytical procedures

2. Ultrasonic spinning rheometry (USR)

2.1 Experimental setup and overview of USR

Experimental setup consisted of an open vertical rotating cylinder made of acrylic resin with 145 mm inner diameter ($2R$) and 65 mm high, 2 mm thick lateral wall (Fig. 1). Cylinder oscillations were controlled at setting oscillation amplitude, $\Theta = \pi/2$ rad, and frequency, $f = 1$ Hz. Instantaneous velocity fluctuations exerted by regular oscillations are measured using UVP, where UVP-model Duo (Met-Flow S.A., Switzerland) was adopted as a velocity measurement system. When velocity vectors in radial direction are negligible compared to the azimuthal component, the azimuthal velocity, u_θ, at a radial position, r, is given as

$$u_\theta = \frac{u_\xi r}{\Delta y}. \qquad (1)$$

Installation of the transducer position, Δy, requires careful handling due to: (1) A much smaller Δy creates significant error and enhances measurement errors. (2) Larger Δy induces an inflection at the cylinder wall due to the large curvature. Since obtained velocity component, u_ξ, contains unavoidable noises due to errors in UVP, it affects the analysis using rheological model, shown in Fig. 1, due to differential amplification of the noises. To overcome the influence, frequency-domain analyses were proposed so

that the obtained data are evaluated without noise influences due to spectral decomposition [5, 7–9].

Yoshida *et al*. [7] developed a method adopting the phase-lag analysis. This method compares the phase lag between the analytical solution and experimental results, so it is possible to quantitatively evaluate the effective Newtonian viscosity. To represent momentum propagations as phase-lag profiles in unsteady shear flows, Tasaka *et al*. [5] derived an analytical solution for spatiotemporal velocity fluctuations of Newtonian fluids. When a unidirectional flow in azimuthal direction is assumed, the Navier-Stokes equation for incompressible fluids is reduced into

$$\frac{\partial u_\theta}{\partial t} = \nu\left(\frac{\partial^2 u_\theta}{\partial r^2} + \frac{1}{r}\frac{\partial u_\theta}{\partial r} - \frac{u_\theta}{r^2}\right), \tag{2}$$

where ν indicates kinematic viscosity of the test fluids. Given appropriate conditions as initial and boundary definitions, an analytical solution is determined. It is derived as $u_\theta = U_{\mathrm{wall}} A(r)\sin[\omega t + \phi(r)]$, where $\omega = 2\pi f$ and $U_{\mathrm{wall}} = 2\pi^2 f R\Theta/180$. The term of $\phi(r)$ is given as

$$\phi(r) = \tan^{-1}\frac{\Phi_R\Psi(r) - \Phi(r)\Psi_R}{\Phi(r)\Phi_R + \Psi(r)\Psi_R}, \tag{3}$$

where the Φ_R, $\Phi(r)$, Ψ_R, and $\Psi(r)$ define terms of infinite series. Further details of the derivation of Eq. (3) are given in [5]. The analytical solution may be adequate in describing unsteady flows in the present system. It has been reported that the phase-lag profile, $\phi(r)$, is in good agreement with experiments using UVP [7].

2.2 Effective Newtonian viscosity measurement

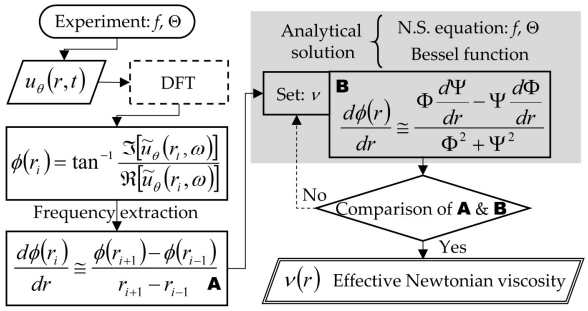

Figure 2: Schematic outline of the analytical process of USR to evaluate "local" effective Newtonian viscosity [7]

Flow diagram of procedure to evaluate rheological property is summarized in Fig. 2. The phase-lag of the velocity fluctuation at a radial point from the cylinder wall was calculated using the discrete Fourier transform (DFT) on the velocity fluctuations. It relates to momentum propagation of the fluid flow depending on its local rheological behavior. Hence, spike-like noises, which is typical of UVP measurements, can almost be removed with the DFT. It was applied to results with an oscillation period, $\Delta t \geq 1$ s, thus this method can track drastic changes in instantaneous viscosity, such as shear thinning, Bingham, and thixotropic fluids. Averaged by N-times measurements in every oscillating cycle periods, the phase-lag profiles are expected to reduce the noises caused by relative errors from UVP. Since there are no results of accuracy in viscosity measurement, accuracy evaluations of the effective Newtonian viscosity measurement are examined by applying numerical solution with artificial random noises to the viscosity measurement explained in §4. A method to generate the random noises assuming the measurement noises is proposed in §3.

3. Noise evaluation in measured velocity

3.1 Statistical calculation for obtained velocity

To obtain velocity fluctuations of unsteady shear flows in silicon oil ($\nu = 1000$ mm^2/s), an ultrasonic transducer of resonance frequency 4 MHz and 5 mm effective element diameter was selected. Important parameters of UVP are temporal resolution $\Delta\tau = 50$ ms, spatial resolution $\Delta\xi = 0.74$ mm, and speed of sound $c = 980$ m/s.

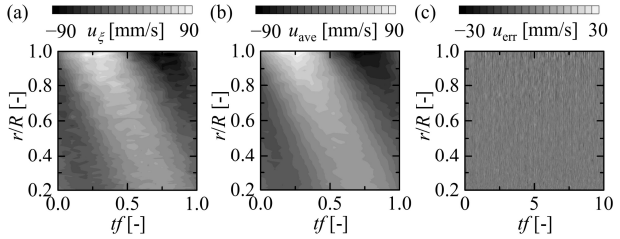

Figure 3: (a) Instantaneous velocity distribution, u_ξ, in experiment, (b) averaged velocity distribution, u_{ave}, with $N = 100$, (c) relative error velocity subtracted u_{ave} from u_ξ

Instantaneous spatiotemporal velocity u_ξ, cycle-averaged velocity u_{ave}, and residual velocity u_{err} are shown in Fig. 3a-c, where the horizontal and vertical axes indicate cycle-period, tf, and radial position normalized by the cylinder radius, r/R. The gray scale indicates velocity amplitude. u_{ave} and u_{err} were calculated by cycle average of u_ξ for $N = 100$ ($\Delta t = 1$ s) and $u_\xi - u_{\mathrm{ave}}$. The velocity fluctuations propagate according with phase-lag from the cylindrical wall, $r/R = 1.0$ (Fig. 3a and b), where the result of Fig. 3a has more noisy profiles than that of Fig. 3b. From u_{err} distribution (Fig. 3c), these noises increase with getting closer to the wall, because quality of velocity obtained by UVP may change depending on velocity magnitude.

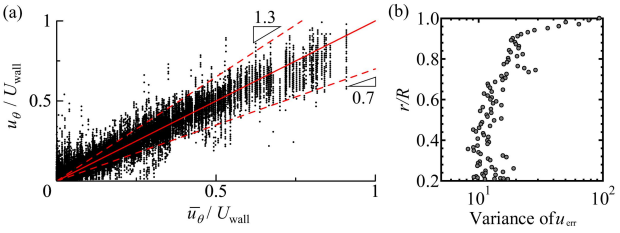

Figure 4: (a) Comparison of instantaneous and averaged velocity, where a total number of plotted data is 2000 × 96, (b) variance profile of u_{err} calculated from Fig. 3c

To confirm factors in the generation of u_{err}, instantaneous velocity was compared to the averaged velocity (Fig. 4a), where differences between u_ξ and u_{ave} were compared in all data of r/R and tf. Two significant findings were observed: (1) Deviations in the measured velocity increase as measurement target velocity increases. (2) Measured velocity profiles have the lowest noise level observed from low velocity in Fig. 4a. Moreover, the variance profile of

u_{err} also indicates the deviation tendency of obtained instantaneous velocity (Fig. 4b), where the horizontal and vertical axes show variance and normalized radial position in the cylindrical container. The variance profiles converged to almost 10 mm^2/s^2 when r/R get closer to the cylinder center. The reason for the significant increase in the variance near the wall is co-reflection of the ultrasound at the interface between acrylic resin the fluid media.

3.2 Production of artificial random noises with normal distribution

Considering the tendency of noises estimated from u_ξ (see Fig. 4), artificial random noises assuming experimental conditions are created by a noise-model function using Box-Muller method [10] to create uniform random values with (0, 1], which are generated by Mersenne Twister [11]. The noises are defined as n (μ, σ^2) with Gaussian distribution, where μ and σ indicate average and standard deviation. The noise-model considered from the experimental result is given as

$$u_{\mathrm{err}} = n_1\left(0, \alpha\left|u_\xi\right|\right) + n_2\left(0, \sigma_{\min}^2\right), \qquad (4)$$

where α and $\sigma_{\min}^2$ indicate a noise amplitude coefficient and the lowest noise level. n_1 and n_2 are a Gaussian random function with normal distribution and are independent of each other. The noise amplitudes were determined by α, included in a function, n_1. On the other hand, the standard deviation of n_2 was determined from the lowest noise level of the experimental result as shown in Fig. 4b. Produced noise at $\alpha = 0.5$ and velocity distribution with noises to the analytical solution are shown in Fig. 5a and b. The produced noises of Fig. 5b are qualitatively agree with that of Fig. 3a. Variance profiles at the case of $\alpha = 0.5$ have good agreement with experimental result (Fig. 5c), so these parameters were determined in §4 to evaluate the accuracy of the viscosity measurement algorithms.

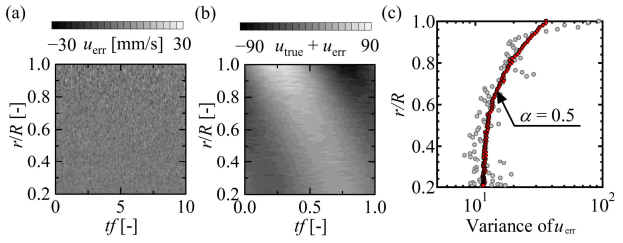

Figure 5: (a) Produced artificial random noises at $\alpha = 0.5$, (b) velocity distribution with noise (a) to velocity calculated form numerical solution, (c) u_{err} variance in noise amplitude $\alpha = 0.5$

4. Accuracy evaluations and improvement

4.1 Phase lag averaging with short time DFT

By utilizing the method to produce velocity distributions by numerical solution with artificial random noises as mentioned above, it is possible to evaluate the accuracy as a probability density distribution P_{vis} (= M_{count}/M) by repetitive computing. M_{count} and M indicate the count number of how many values fall into each bin and number of trials. P_{vis} is calculated by numerical computation with $M = 2000$. Histograms of simulated results were calculated by counting M_{count} at every step of ν in 20 mm^2/s from 0 mm^2/s to 2000 mm^2/s. Probability density distribution of viscosity profiles was evaluated from simulated velocity distribution at cases of averaging cycle times, $N = 1$, 80, 320 (Fig. 6). The horizontal and vertical axes indicate kinematic viscosity and normalized radial position, where the true value of kinematic viscosity to solve the analytical solution is emphasized by the dashed line. The gray scale shows the probability of viscosity measurement using the phase-lag analysis. To evaluate the viscosity profiles, phase lag obtained from the velocity distribution is needed to calculate the differential. Noises in the phase lag influences viscosity measurements due to noise amplification of differential in phase-lag profiles. So, before the calculations are processed, noise reductions of phase-lag profiles are required to reduce viscosity scattering. When the phase-lag profiles are $N = 1$, the evaluated viscosity profiles are scattered with large difference from the true value (Fig. 6a). Since the noises in phase-lag profiles decreases by calculating arithmetic mean profiles in $N > 1$, histograms of the viscosity show higher accuracy and precision than that of $N = 1$ (Fig. 6b and c).

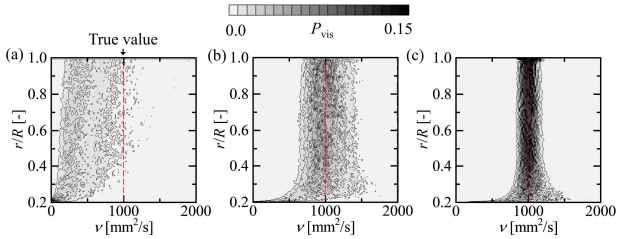

Figure 6: Histogram in probability density distribution of the viscosity at cases (a) $N = 1$, (b) $N = 80$, (c) $N = 320$

At noise amplitudes in different N, mode value (highest probability density distribution), +25% summation of the distribution from the mode value, and −25% of that are summarized in Table 1, where these results were averaged by $0.6 < r/R < 1.0$ and obtained from the viscosity. It indicates the accuracy of the viscosity depending on the averaging cycle times N. Arithmetic mean calculations are, however, limited when test fluids have constant rheological properties with changing shear rate (Newtonian fluid).

Table 1: Mode, +25%, and −25% values calculated from histograms of the viscosity, which are averaged by $0.6 < r/R < 1.0$

N	1	20	40	80	160	320
Mode [mm^2/s]	316	919	938	965	981	993
+25% [mm^2/s]	684	1122	1083	1051	1040	1032
−25% [mm^2/s]	-	695	754	818	919	952

4.2 Spectral subtraction method utilizing periodic functionalized algorithm

Considering noise reductions in phase-lag profiles obtained from instantaneous velocity fluctuations, it is expected that spectral subtraction method utilizing periodic functionalized algorithm is efficient. A restricting condition in both ends of the phase-lag profiles was given to apply the DFT filtering for the phase-lag profiles. The condition is a periodic functionalized formula, φ, which is defined as following formula (schematic details in Fig. 7a):

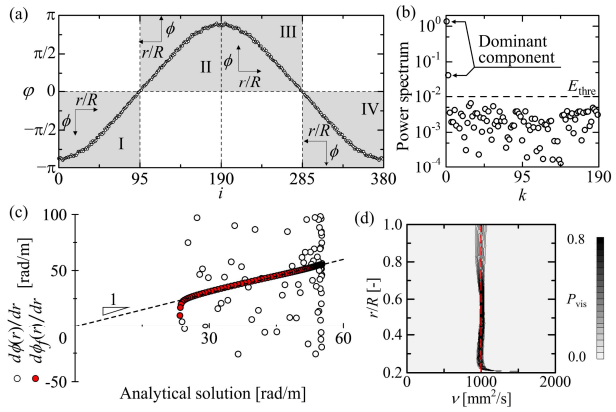

Figure 7: (a) Periodic function defined in Eq. 5, (b) power spectrum obtained from periodic function, (c) analytical solution versus spatial gradient of $\phi(r)$ and $\phi_f(r)$, (d) probability density distribution of the measurement from filtered phase-lag profiles

$$\varphi(i)=\begin{cases}-\phi_{X-i-1} & (\mathrm{I}: 0\le i<X)\\ \phi_{i-X+1} & (\mathrm{II}: X\le i<2X-1)\\ \phi_{3X-i-2} & (\mathrm{III}: 2X-1\le i<3X-2)\\ -\phi_{i-3X+3} & (\mathrm{IV}: 3X-2\le i<4X-4)\end{cases} \quad (5)$$

X indicates a total number of radial profiles. Power spectra in $\varphi(i)$ calculated by DFT have dominant Fourier components (Fig. 7b), where the power smaller than E_{thre} (= 10^{-2}) are regarded as additive noise components due to white noise characteristics. Removing the noise components on the spectra, the original phase-lag profiles $\phi(r)$ were filtered by inverse DFT. Comparing analytical solution with spatial gradients obtained from filtered phase-lag profiles $\phi_f(r)$ and $\phi(r)$, gradients of the filtered profiles are better agreement with the analytical solution than that of original profiles (Fig. 7c). By using this filtering process, the probability density distributions (Fig. 7d) indicate higher accuracy compared to the original histogram shown in Fig. 6a.

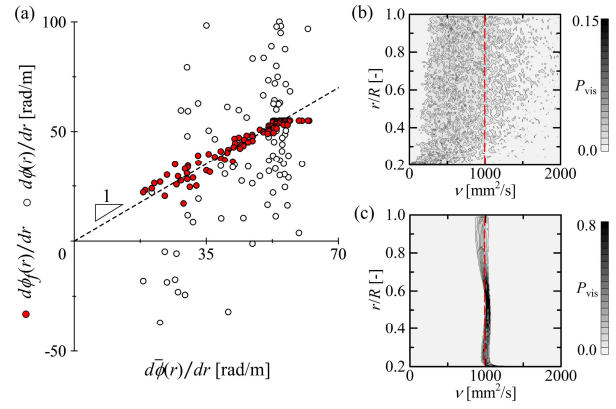

Figure 8: (a) Spatial gradient of $\bar{\phi}(r)$ versus $\phi(r)$ and $\phi_f(r)$ at each radial position, and probability density distribution of viscosity measurement from (b)$\phi(r)$ and (c)$\phi_f(r)$ in $\Delta t = 1$ s ($N = 500$) of viscosity measurement

Actual measurement results (silicon oil: 1000 mm^2/s) were analyzed to confirm the applicability of this spectral subtraction method. $d\phi(r)/dr$ and $d\phi_f(r)/dr$ obtained from $N = 1$ were compared with $d\bar{\phi}(r)/dr$ (Fig. 8a), where $\bar{\phi}(r)$ was averaged by $N = 500$ times of phase-lag profiles. $d\phi_f(r)/dr$ has a correlation with $d\bar{\phi}(r)/dr$ compared to $d\phi(r)/dr$, therefore this filtering method can reduce the noises equal to or greater than the arithmetic mean calculation. Probability density distributions of the kinematic viscosity obtained from $d\phi(r)/dr$ and $d\phi_f(r)/dr$ were evaluated as shown in Fig. 8b and c. The precision of viscosity measurement from $\phi_f(r)$ became higher than that of $\phi(r)$, although silicon oil may not be given accurate kinematic viscosity value due to fluid quality and temperature control.

5. Summary

We estimated the accuracy of the rheological evaluation using phase-lag analysis. Artificial random noises with the normal distribution, which can represent actual velocity by estimating experimental noises in UVP, were produced. This production of artificial random noises can realize statistical evaluations from numerical calculations. Thus, it is possible to estimate the accuracy of the measurement system by iterative computing. The measurement noises of viscosity were caused by the noise of differential amplification in phase-lag profiles. To apply the spectral subtraction to the phase-lag profiles, the additive noises can be eliminated. These results were obtained from $N = 1$ ($\Delta t = 1$ s), so the filtering process is expected to be applied to complex fluids with instantaneously changeable rheological properties, such as polymer solutions, thixotro-pic fluids, and bubbly liquids. This can lead to highly accurate and real-time rheometry. As future prospects, the accuracy of another analytical procedure in USR will be validated by the iterative calculation using the artificial random noises assuming actual measurement errors.

References

[1] Divoux T, *et al.*: Shear banding of complex fluids, Annu. Rev. Fluid Mech., 45 (2016), 81−103.
[2] Takeda Y: Ultrasonic Doppler velocity profiler for fluid flow, Springer (2012).
[3] Shiratori T, *et al.*: Development of ultrasonic visualizer for capturing the characteristics of viscoelastic fluids, J. Vis., 16.4 (2013), 275−286.
[4] Shiratori T, *et al.*: Ultrasonic velocity profiling rheometry based on a widened circular Couette flow, Meas. Sci. Technol., 26 (2015), 085302.
[5] Tasaka Y, *et al.*: Estimating the effective viscosity of bubble suspensions in oscillatory shear flows by means of ultrasonic spinning rheometry, Exp. Fluids, 56 (2015), 1867.
[6] Shiratori T *et al.*: Rapid rheological characterization of a viscoelastic fluid based on spatiotemporal flow velocimetry, Exp. Therm. Fluid Sci., 71 (2016), 1−13.
[7] Yoshida T, *et al.*: Rheological evaluation of complex fluids using ultrasonic spinning rheometry in an open container, J. Rheol., 61.3 (2017), 537−549.
[8] Tasaka Y, *et al.*: Linear viscoelastic analysis using frequency-domain algorithm on oscillating circular shear flows for bubble suspensions, Rheologica Acta, 57.3 (2018), 229−240.
[9] Yoshida T, *et al.*: Rheological properties of montmorillonite dispersions in dilute NaCl concentration investigated by ultrasonic spinning rheometry. Appl. Clay Sci., 161 (2018), 513−523.
[10] Box GEP, *et al.*: A note on the generation of random normal deviates. Annu. Math. Statist., 29.2 (1958), 610-611.
[11] Matsumoto M and Nishimura T: Mersenne twister: a 623-dimensionally equidistributed uniform pseudo-random number generator, ACM TOMACS, 8.1 (1998), 3−30.